High Energy Tests of QCD

Gerald C. Blazey

Northern Illinois University
DeKalb, Illinois 60115

Abstract. Selected, recent, high energy results, primarily from collider experiments but including some fixed target experiments, are presented as illustrations of the status of Quantum ChromoDynamics (QCD). The concepts of leading order (LO) and next–to–leading order (NLO) QCD are introduced. Inclusive $\bar{p}p$ jet production as a function of jet transverse energy and cone size and di–jet angular distributions are shown to be in reasonable agreement with QCD. Jet shapes from $\bar{p}p$, ep, and e^+e^- colliders are also compared to NLO QCD. Discrepancies between NLO calculations and data are apparent for measurements which involve a clearly identified final state parton. This is demonstrated by an unexpectedly large ratio of W+1–jet production to W+0–jet production and an unexpectedly large b–quark cross section in $\bar{p}p$ scattering. Similarly, a compilation of $\bar{p}p$, pp, and fixed target scattering results shows prompt photon production to be systematically greater than NLO predictions. Measurements of the Casimir color factors and the strong coupling constant (α_s) are presented and are in good agreement with theoretical expectations. The decrease of α_s with momentum transfer is apparent in a compilation of world results. New measurements of α_s from e^+e^-, ep, and fixed target experiments do not affect the world average $\alpha_s = 0.118 \pm 0.003$.

INTRODUCTION

The field of high energy quantum chromodynamics (QCD) is in a period of great excitement and rapid advance. Results from three complementary high energy colliders ($\bar{p}p$, ep, e^+e^-) as well as fixed target experiments are providing a broad and comprehensive view of experimental QCD. This, in turn, has stimulated a great deal of theoretical work and progress in the field. For example, measurements of jet production and semi–inclusive W+jet, photon, and heavy quark production illustrate the breath of experimental progress. Although theoretical calculations adequately describe most aspects of jet production, they fall short of describing the semi–inclusive measurements. On a more fundamental level, there has been great improvement in determination of basic QCD parameters involving the quark and gluon couplings. These increasingly more accurate and complete measurements are testing the limits and applications of QCD.

The proton–antiproton interaction, a fairly general scattering process, nicely introduces the concepts of leading order and next–to-leading order QCD. As shown in Fig. 1, hadron–hadron scattering can be considered a convolution of

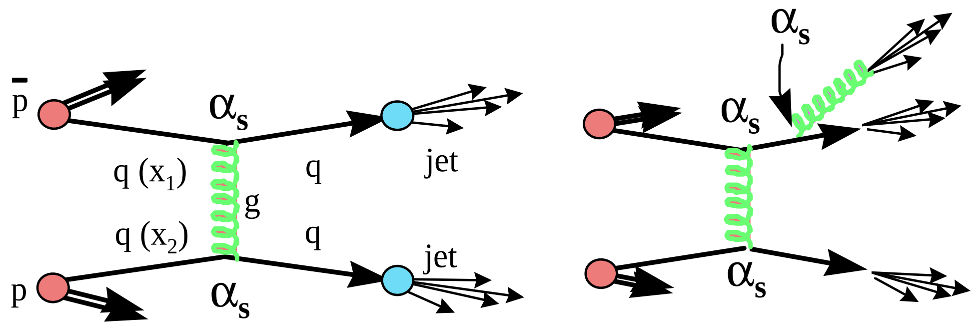

FIGURE 1. Factorization of the scattering process: Incoming quarks with momentum fraction x_i of the incident hadrons scatter through gluon exchange and fragment into final state jets.

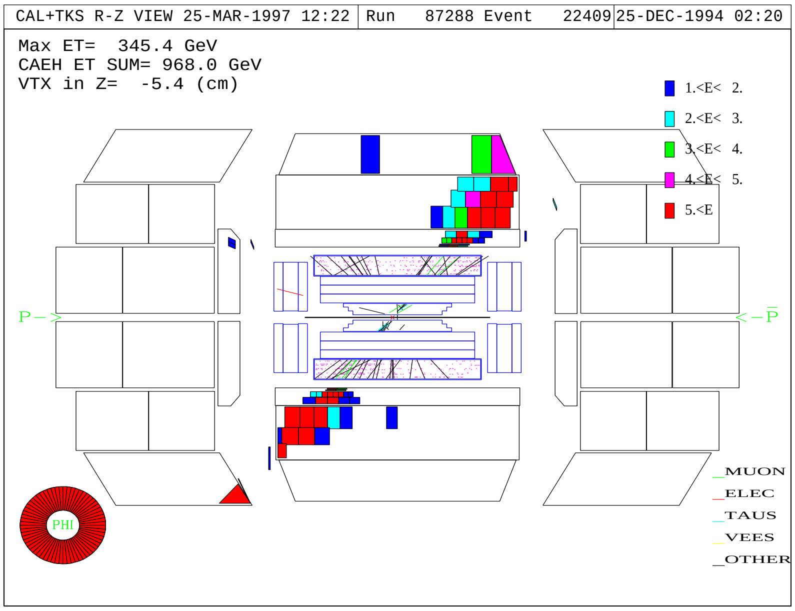

FIGURE 2. A high energy two jet event.

parton distribution functions, a hard two–body interaction, and nonperturbative fragmentation or hadronization functions. The nonperturbative parton distribution function (pdf) for each incoming particle $q(x_i)$, describes the momentum fraction, x_i, carried by each constituent or parton of the parent hadron. The hard two–body interaction, $\hat{\sigma}$, between quarks and gluons is described by perturbative QCD. The figure depicts $qq \to qq$ elastic scattering. In general, pdf's describe the gluon, quark, and antiquark contents of protons, and the hard scattering describes interactions between the partons. The nonpeturbative fragmentation or hadronization function, d, represents the manifestation of the final state quarks and gluons as observed particles. The cross section for the process in Fig. 1 can be written succinctly as $\sigma = \int q(x_1)q(x_2)\hat{\sigma}_{12}d_1 d_2$.

The factorized scattering has been illustrated with a leading order graph; that is, a graph proportional to two powers of the strong coupling constant, α_s. A good experimental example of such a leading order process is shown in Fig. 2. This represents a proton–antiproton collision recorded by the DØ [1] detector at the Fermi National Laboratory Tevatron Collider in Batavia, Illinois. The incoming beam energies are 900 GeV/c (center of mass energy 1800 GeV/c). At leading order, the scattering can be understood as a quark from the proton scattering elastically off an antiquark from the antiproton. The final state partons then fragment and hadronize as showers or jets of energy seen in the detector. The two final state jets have energy transverse to the beam axis, E_T , of 480 GeV/c and are the highest transverse energy jet pair observed. Note that the final state jets are considered equivalent to the final state partons.

Although useful the leading order picture is too simple. Current next–to-leading order (NLO) or O(α_s^3) calculations include radiative corrections or additional gluon emission. This is shown in the second illustration of Fig. 1, here a final state parton has radiated an additional gluon and so the entire scattering process is proportional to α_s^3. The final state radiation in the hard scatter can be thought of as a replacement for the fragmentation functions so that $\sigma = \int q(x_1)q(x_2)\hat{\sigma}_{12}$. At this point a technical note is warranted: The perturbative expansion of $\hat{\sigma}$ must be evaluated at some momentum transfer which is typically taken to be the momentum transfer between the partons, errors incurred in the theoretical prediction due to this choice are of O(α_s^4). To a large degree current high energy QCD is simply a study of the additional radiation. As shown in the next section this is well illustrated by jet production in the high energy regime. (Measurement and determination of the parton distribution functions and hadronization functions are each vast and interesting topics of discussion. See the talk by U. Straumann in these proceedings for details on parton distributions.)

JET PRODUCTION

The Inclusive Jet Cross Section

A complete theoretical description of inclusive jet production, $p\bar{p} \to j + X$, requires proper treatment of the final state radiation and accurate measurements of the parton distribution functions, pdf's. Thus the inclusive cross section is a basic test of perturbative NLO QCD as well as the pdf's. Perhaps most interestingly, with current data sets, the inclusive jet cross section constitutes a search for new physics at a distance scale of 10^{-17} cm. In a manner completely analogous to Rutherford scattering, excess jet production at very large transverse energies signals the presence of quark compositeness.

The cross section is typically reported as $d^2\eta/dE_T d\eta$. $E_T = Esin\theta$ where E is jet energy and θ the angle between the proton direction and the jet. The pseudorapidity, η, is defined as $-ln(tan(\theta/2))$. Kinematically, an individual jet is characterized by E_T , η, and ϕ where ϕ is the azimuthal direction of the jets. At ninety degrees to the beam line the jet energy is equal to E_T and the pseudorapidity is zero. As the jet nears the beam axis in the forward or backward direction the magnitude of η grows. Jets are found by clustering energy in a cone of radius $R = 0.7$ in $\eta - \phi$ space.

Figure 3 shows the central inclusive jet cross section as measured by the DØ collaboration at beam energies of 900 GeV/c for $|\eta| < 0.5$ [2]. The data

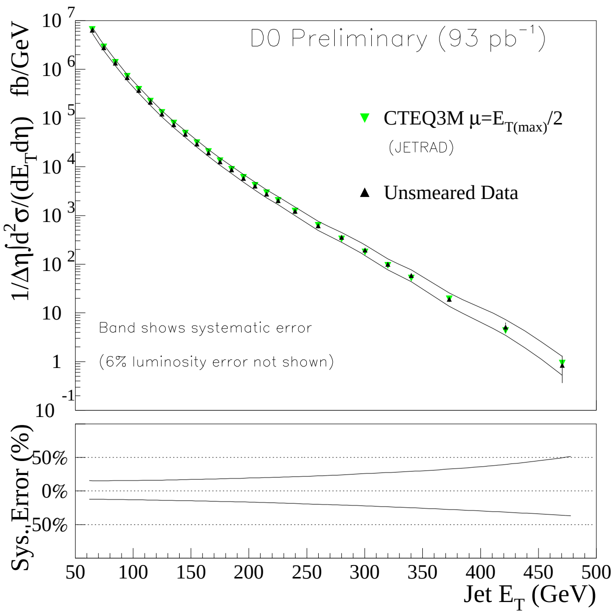

FIGURE 3. The central inclusive jet cross section.

spans seven orders of magnitude for jet energies between 50 and 450 GeV. Data points include statistical errors only and the inset indicates the magnitude of the systematic errors. The systematic error is dominated by uncertainties in the jet energy scale. The figure includes a NLO prediction due to Giele, Glover and Kosower [3]. The cross section has also been calculated by Ellis, Kuntz and Soper [4]. The percentage difference as a function of E_T between the data and theory is shown in Fig. 4. Note there is excellent agreement at all E_T and no indication of new physics.

As shown in Fig. 5 the CDF experiment [5] shows a similar result below 200 GeV for jets in the region $0.1 < |\eta| < 0.7$. However, there is a clear discrepancy at high energy. The open symbols represent published data from a 1992-1993 data run [6]. The closed circles represent a high statistics 1994-1995 data run [7]. The CDF systematic errors (slightly better than those shown in Fig. 3) cannot explain the high energy discrepancy with NLO QCD.

A direct comparison of CDF data to DØ data in the region $0.1 < |\eta| < 0.7$ shows the two experiments to be consistent within systematic errors. The CDF result is roughly 10–20% above the DØ result with a 10% dependence on E_T . Despite the experimental agreement, the two theoretical comparisons suggest differing levels of agreement with NLO QCD. The apparent discrepancy can be attributed to different parameter selections for the NLO predictions. Each theoretical prediction requires a choice of pdf, renormaliza-

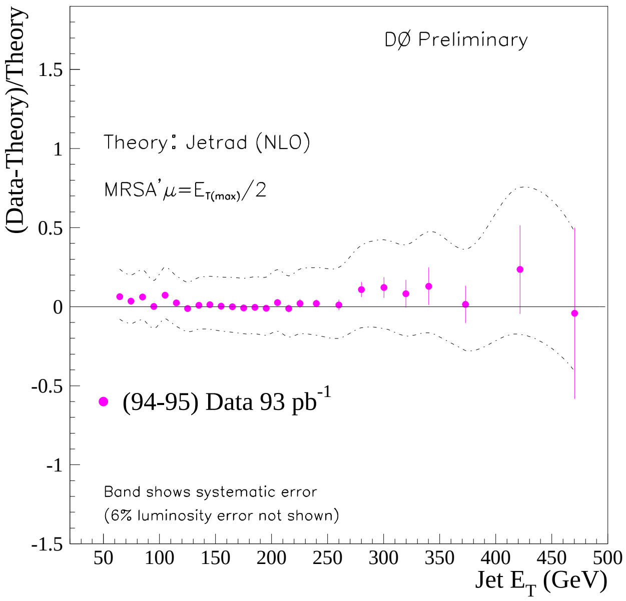

FIGURE 4. Difference between data and NLO QCD for the central inclusive jet cross section as measured by DØ .

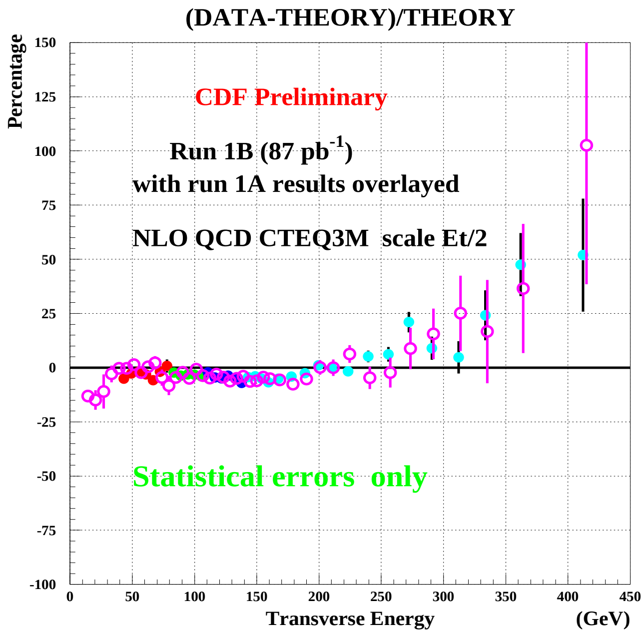

FIGURE 5. Difference between data and NLO QCD for the central inclusive jet cross section as measured by CDF.

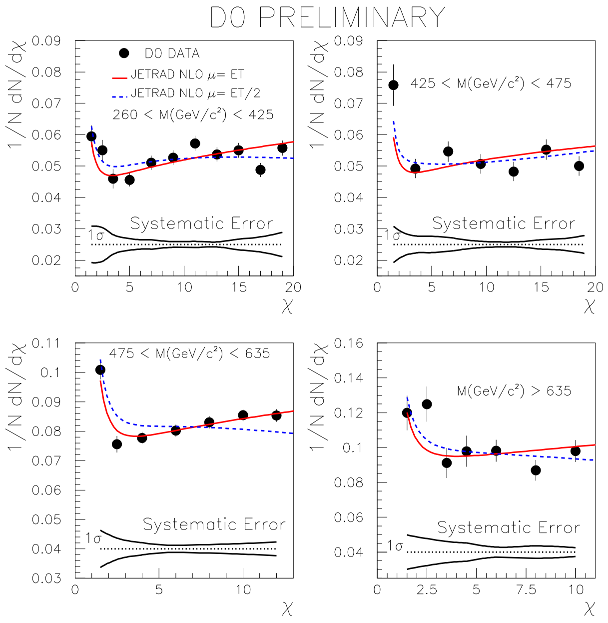

FIGURE 6. Dijet angular distributions.

tion scale, and parton clustering algorithms. The pdf, scale, and clustering choice can engender 15%, 10%, and 3% variations in the NLO prediction. The DØ comparison in Fig. 4 incorporates the MRSA' pdf [8] and a renormalization scale of Et(max)/2 where Et(max) represents the maximum jet E_T in an event. The CDF comparison incorporates the MRSA' pdf and a renormalization scale of Et/2 where Et represents jet E_T . Further clarification of the theoretical comparison awaits more accurate measurements of the pdf's, higher order calculations to reduce renormalization and clustering uncertainties, and a reduction of systematic errors. Nonetheless within 15-20% NLO QCD describes the inclusive jet cross section over eight orders of magnitude.

Dijet Angular Distributions

Angular distributions between the leading two jets of a hard $\bar{p}p$ event also constitute a rigorous test of NLO QCD. In the lab frame, the two jets are produced at rapidities η_1, η_2. When boosted into the center–of–mass the jets or partons will be at opposite rapidity $\eta_1' = -\eta_2'$ so that the hard scatter is characterized by the angle, θ^*, between the leading jet and the direction of the proton beam. Typically, the angular distribution is plotted in the normalized form $(1/N_{jets}) \times dN/d\chi$ where $\chi = (1 + cos\theta^*)/(1 - cos\theta^*)$. Since $\chi \sim 1/sin^4(\theta^*/2)$, $dN/d\chi$ is flat for Rutherford scattering. Fig. 6 illustrates the remarkable agreement between measured angular distributions and NLO QCD for four dijet mass bins [2]. The data shows a preference for NLO over LO QCD. This indicates proper treatment of the radiative corrections is required to describe the angular distributions.

The highest mass region is also quite sensitive to new physics in the form of a contact interaction or constituent exchange between scattering quarks. As with the inclusive cross section, additional contributions will enhance production at ninety degrees to the beam line or at $\chi \sim 1$. Because gg, gq, and qq scattering processes all have very similar angular distributions, the dijet angular distribution is quite insensitive to input pdf's. Thus, deviations from QCD expectations will not be obscured by pdf uncertainties. This is in contrast to a compositeness search with the inclusive jet cross section. The high mass χ distributions can be compared to NLO QCD predictions with and without composite interactions to set lower limits on quark compositeness [2], [9]. The current best limit of 2.3 TeV indicates that for the case of dijet angular distributions there is no indication of new physics.

Jet Shape

The inclusive $\bar{p}p$ cross section can also be measured as a function of cone size [10], [11]. Of particular interest is the ratio of the cross section for various cone sizes as a function of jet E_T [10]. The ratio of the 1.0 cone cross section to the

0.7 cross section and the 0.5 to the 0.7 cross section, for example, shows the cross section to increase with cone size. Above $E_T = 80$ GeV/c the ratios are in good agreement with NLO QCD. Since the theoretical calculations indicate that there is little dependence of the ratios on the pdf's, NLO QCD accurately predicts gluon emission characteristics.

Closely related to the variance of the inclusive cross section with cone size is jet shape or energy flow profile. Quantitatively this may be defined as $\Psi(r) = \Sigma(E_T(< r)/E_T(< R = 1))/N_{jets}$. The function $\Psi(r)$ reflects the sum of the transverse energy within a subcone r normalized to the total energy within the cone $R = 1$. Qualitatively, Ψ will rise to unity rapidly for a thin jet and slowly for a fat jet. To describe jet shape a new parameter must be added to NLO theory. The parameter, D, sets the maximum distance between partons clustered into a final state jet. For example, partons within a distance D=1 in $\eta - \phi$ space may be clustered into a single jet and those more than D=1 apart remain unclustered. Thus, at NLO a single event may include one, two, or three jets.

Jets shapes or transverse energy flow for jets produced at the Tevatron collider and at LEP, the e^+e^- collider in Geneva, Switzerland, can be found in the literature [12]. Jet production at the Tevatron is well described by the single additional gluon of NLO QCD with D $\sim$1 . At comparable jet energies, since Tevatron jets are dominated by gluons (from gg elastic scattering) and LEP jets by quarks (from pair creation) and since gluons radiate more than quarks, QCD predicts that Tevatron jets will be “fatter” than LEP jets. In fact, very beautiful analyses of LEP three jet events clearly demonstrate that u, d, and s quark jets are narrower than gluon jets [13].

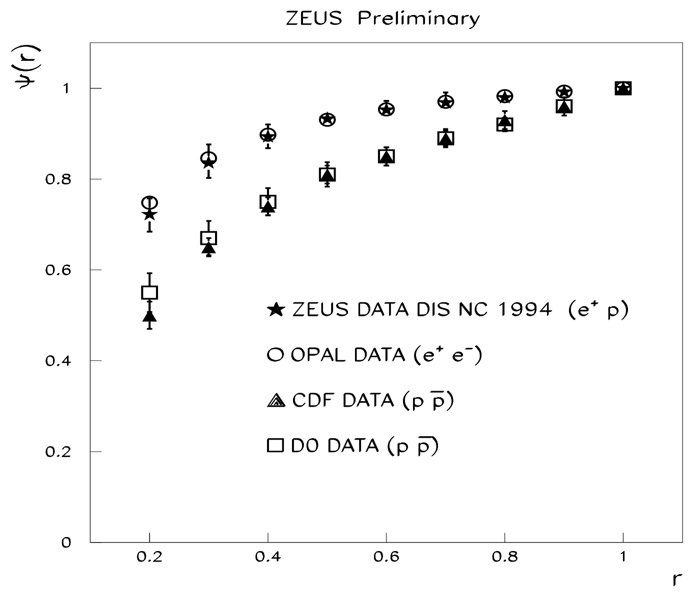

FIGURE 7. Jet shapes from various colliders.

With recent results from HERA, the electron–proton collider in Hamburg, Germany, jet shapes can be compared for all three colliders. For momentum transfer, Q^2, greater than 100 GeV^2, ep scattering is dominated by photon exchange between the incident electron and struck quark. As a result, the final state partons always include a quark. At comparable energies then, QCD predicts that LEP and HERA jets will have similar profiles. The similarity is clearly demonstrated in Fig. 7 [14]. The stars show the jet energy profile as measured by the ZUES collaboration at HERA for a positron beam energy of 28 GeV and a proton energy of 820 GeV. The jet E_T is between 37 and 45 GeV. The results track neatly the LEP profile as measured by the OPAL collaboration for jet energy less than 35 GeV and beam energy of 45 GeV.

Although not shown, the HERA jets shapes can be described by NLO QCD in all kinematic regions if the parton distance variable, D, is allowed to vary between 1 and 1.5 [15]. The other two data curves in Fig. 7 correspond to jets as measured by CDF ($40 < E_T < 60$ GeV) and DØ ($45 < E_T < 75$ GeV) at the Tevatron. As expected because of gluon dominance the Tevatron jets are "fatter" than LEP and HERA jets. Apparently, jet structure seems to be universal or independent of environment and surprisingly well described by single gluon emission or $O(\alpha_s)$ calculations.

SEMI–INCLUSIVE PRODUCTION

W+jet

To lowest order, W production at the Tevatron $\bar{p}p$ collider involves only an electroweak vertex and is unaccompanied by partons or jets. When an additional parton or jet is produced through annihilation ($q\bar{q}' \rightarrow Wg$) or Compton scattering ($qg \rightarrow W\bar{q}'$), an additional factor of α_s enters the picture. Current QCD calculations are exact to order α_s^2 and describe the emission of an additional gluon. In the cases of annihilation or Compton scattering, the final state gluon or quark may radiate.

Since systematic uncertainties cancel, a particularly useful test of NLO QCD is given by the ratio of W+1–jet production to W+0–jet production, R^{10}. Both the lowest order and $O(\alpha_s)$ processes contribute to W+0–jet production and the $O(\alpha_s)$ and $O(\alpha_s^2)$ processes to the W+1–jet production. The ratio has been calculated to $O(\alpha_s^2)$ by Giele, Glover and Kosower [16]. Figure 8 shows the theoretical calculation to be a factor of two or more below the measurement at all jet E_T [17]. Jets are counted as a function of a minimum threshold E_{Tmin}. The two theoretical curves differ only by the choice of pdf and demonstrate that pdf uncertainties cannot explain the discrepancy. As with the NLO jet comparisons, uncertainties due to the choice of the renormalization scale and parton clustering are small ($\sim 10\%$). The R^{10} discrepancy represents the first of several inconsistencies between NLO QCD and semi–inclusive processes (processes in which at least one of the final state partons is clearly identified).

Heavy Quarks

Heavy quark production ($\sigma_{t\bar{t}}, \sigma_{b\bar{b}}$) in hadron–hadron scattering provides another important test of NLO QCD. At leading order, heavy quarks are produced primarily through valence quark annihilation and subsequent pair creation. In the case of top production at Tevatron energies, NLO corrections are dominated by gluon radiation from the final state t or $\bar{t}$ [18]. Current NLO predictions for the top cross section , $4.7 - 5.5$ pb for a mass of 175 GeV are in good agreement with measurements from the CDF and DØ collaborations, $7.5^{+1.9}_{-1.6}$ pb for a mass of 175 GeV and 5.5 ± 1.8 pb for a mass of 173 GeV, respectively [19]. The top cross section will not be a precise test of QCD until Tevatron Run II when statistical samples increase tenfold.

Interestingly, NLO corrections for $b\bar{b}$ production are of the same order as LO contributions. This can be attributed to "gluon splitting" in which valence quark annihilation leads to two final state gluons, one of which splits into a $b\bar{b}$ pair. The b quark cross section has been measured in many semi–inclusive channels. These include observation of the muon p_T spectrum from the semi–leptonic decays of the b quarks with or without jets, from dimuon final states,

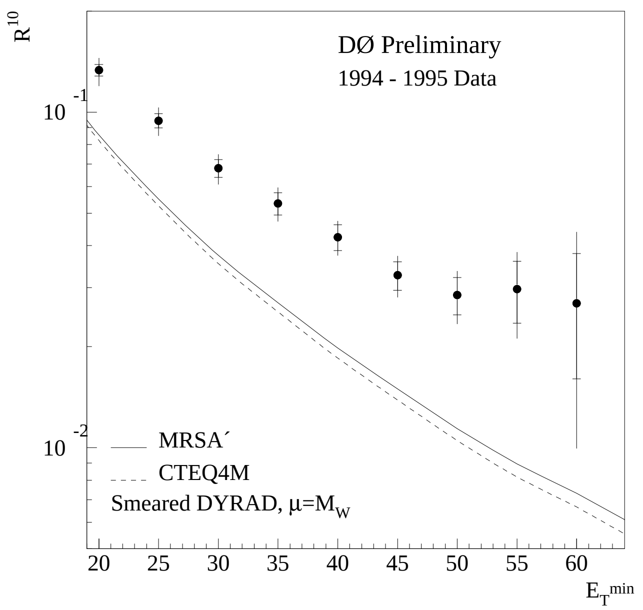

FIGURE 8. Ratio between W+1jet and W+0jet production.

and from meson resonances. Experimental measures of $\sigma_{b\bar{b}}$ as a function of the b quark p_T are well above the nominal NLO predictions [20].

The Photon Cross Section and "k_T"

At leading order direct photon production can occur by annihilation, $q\bar{q} \to g\gamma$, and by Compton scattering, $qg \to q\gamma$ or $\bar{q}g \to \bar{q}\gamma$, and is therefore quite sensitive to the gluonic content of the proton. Higher order bremsstrahlung graphs, for instance $qg \to qg$ where the final state quark radiates a photon, also provide beyond–leading–order tests of QCD. Inclusive photon measurements are free of uncertainties due to jet energy scale and reconstruction. Likewise, theoretical calculations are not hampered by parton clustering algorithms. The measurement does suffer one important drawback: the signal must be extracted from the large π^0 and η meson decay background. There are several methods employed to reduce or estimate the background and details can be found in the references [21]. Nevertheless, because the photon and jet based measurements have very different systematic errors, they provide important complementary tests of QCD.

The CTEQ collaboration has noted an excess of photon production at low x in nearly all the direct photon data accumulated over the last ten years [23]. Figure 9 plots the percentage difference between the NLO predictions for inclusive production and the data for an impressive array of results. The

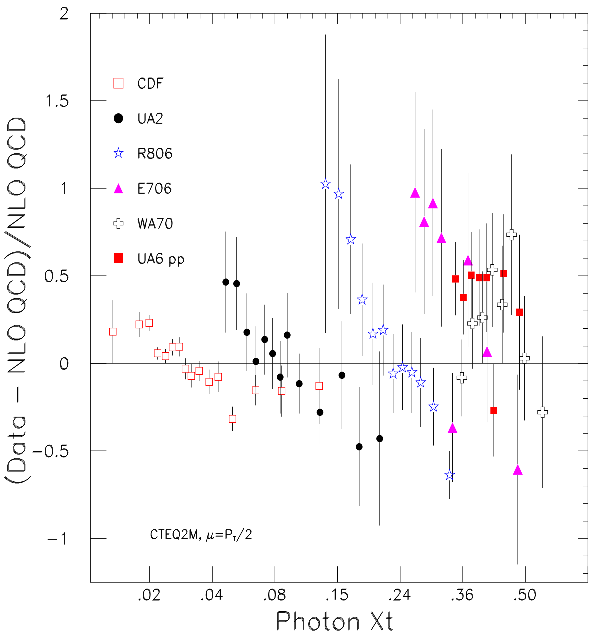

FIGURE 9. Compilation of direct photon measurements compare to NLO QCD.

curve is plotted versus photon $x_t = 2p_T/\sqrt{s}$ where p_T is the photon transverse momentum and s the center of mass energy. At the lowest x accessible by each experiment there appears to be excess production. A NLO prediction using all the photon data to determine the pdf shows nearly identical behavior.

A possible origin of the excess, as suggested by CTEQ, could be higher order processes which impart transverse momentum or "k_T" to the initial partons. The presence of such transverse momenta on the observed cross section would be profound. Since the k_T would be misinterpreted as p_T, the observed cross section as a function of p_T would be a smeared version of the true cross section as a function of p_T. The high cross section at lower p_T would make a large contribution at higher p_T's.

Supporting evidence for nonzero k_T can be found in diphoton production data in hadron colliders [24]. In all cases, the average p_T of the diphoton system is nonzero. At the Tevatron the average is $\sim$ 4 GeV/c. Detailed simulations show this to be the correct magnitude required to explain the excess production at low p_T. Finally, theoretical predictions for prompt photon production from pBe fixed target scattering at $\sqrt{s}$ =31.6 GeV/c are a factor two low unless an average k_T of 1.3 GeV/c is included in the calculation [22]. The "k_T" requirement is most assuredly an interesting observation; higher order calculations may be required to explain these results.

QCD PARAMETERS

Casimir Factors

The only free parameter of QCD is the strong coupling constant α_s. However, the relative strengths of the three distinct quark and gluon vertices, $\alpha_s C_F$ for $q \to qg$, $\alpha_s C_A$ for $g \to gg$, and $\alpha_s T_F$ for $g \to q\bar{q}$ are completely determined by the structure of the gauge group describing the strong force. For $SU(N_c)$ where N_c is the number of colors $C_A = N_c$, $C_F = (N_C^2 - 1)/2N_C$, and $T_F = 1/2$. The probability for a gluon to radiate a gluon is roughly twice the probability for a quark to radiate a gluon. (This is reflected in the narrowness of quark jets discussed earlier.) Four jet production in e^+e^- scattering provides a beautiful experimental measurement of these color or Casimir factors and so a direct test of the gauge couplings [25].

All three of the basic vertices are present in four jet production: the two final state quarks may each radiate a gluon, one quark may radiate two successive gluons, a single quark may radiate one gluon which splits into two gluons, or a single quark may radiate one gluon which splits into a quark–antiquark pair. Since each diagram involves spin–1 and spin–1/2 particles in different configurations each graph results in different angular distributions for the final states. Thus, the observed four jet angular distributions can be fit to theoretical predictions with C_F, C_A, and T_F as free variables.

Figure 10 shows the results of a recent analysis from data taken at LEP (beam energy 45 GeV) by the ALEPH collaboration [25]. Ratios of the Casimir factors are taken to remove sensitivity to the strong coupling constant. Note the 65% contour eliminates many possible gauge groups and comfortably encompasses SU(3). The most probable values of $C_A/C_F = 2.20 \pm 0.16$ and $T_F/C_F = 0.29 \pm 0.08$ compare quite well with SU(3) expectations of 2.25 and 0.375, respectively. Also shown are results from similar analyses by OPAL and DELPHI.

The Strong Coupling Constant

An enormous body of research has been dedicated to the study of the strong coupling constant, α_s since it is the only free parameter of QCD and must be

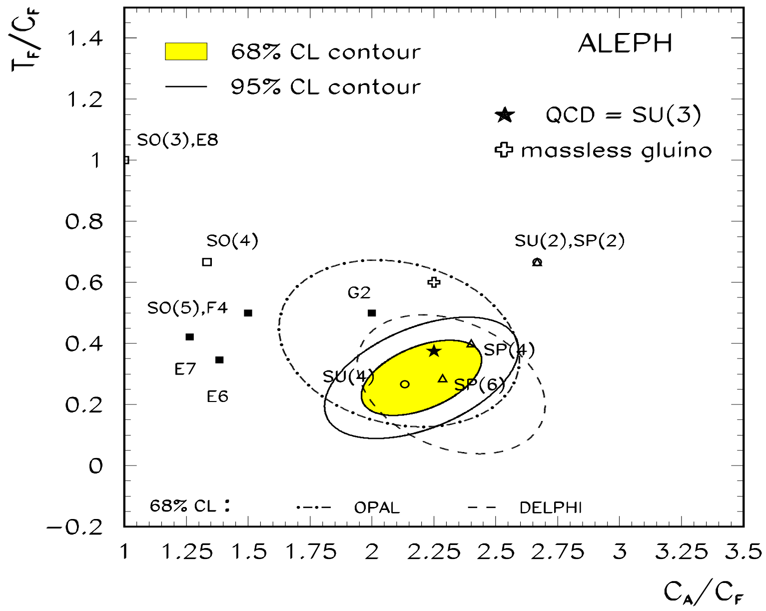

FIGURE 10. Contour plot for Casimir factors measured with 4–jet events.

determined experimentally. Of equal interest is the dependence of the coupling constant on momentum transfer Q^2, $\alpha_s(Q^2) = 12\pi/(33-n_f)log(Q^2/\Lambda^2)$ where n_f is the number of quark flavors and Λ is experimentally determined. Notice α_s decreases or "runs" with momentum transfer. This is, in fact, the basis for the perturbative NLO QCD calculations described earlier. By convention α_s is reported at momentum transfer equal to the Z mass.

The strong coupling constant can be derived in a myriad of ways, from absolute decay rates of the Z boson and τ lepton, energy levels of bound heavy quarks, jet event shapes, jet production rates and angular distributions, and scaling violations in deep inelastic scattering. Details of these derivations can be found in the many references on the strong coupling constant. Figure 11, taken from the excellent, recent review by M.Schmelling, is a compilation of some of the many derivations of α_s and is a beautiful demonstration of running [26]. The curves are derived from the evolution of α_s using the running equation and the world average, $\alpha_s(M_Z) = 0.118 \pm 0.003$. Note that the strong coupling constant is known to three percent accuracy.

The plot does not include some of the most recent results from LEP, the CCFR neutrino scattering experiment, and HERA. In particular, LEP recently ran at center–of–mass energies of 133, 161, and 172 GeV and from event shape measurements determined $\alpha_s(133GeV) = 0.113 \pm 0.003 \pm 0.007$, $\alpha_s(161GeV) = 0.105 \pm 0.003 \pm 0.006$, and $\alpha_s(172GeV) = 0.103 \pm 0.003 \pm 0.006$ where the first error is statistical and the second theoretical [27]. Recent

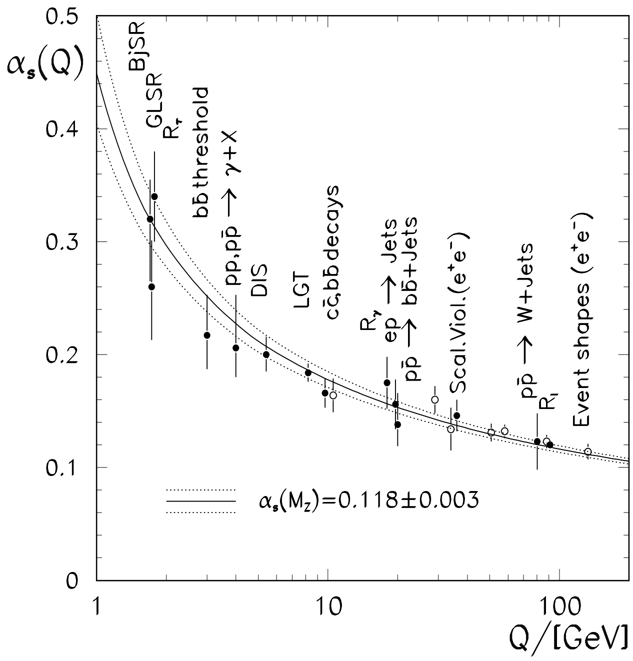

FIGURE 11. A compilation of α_s measurements.

jet event shape results from the H1 collaboration experiment at HERA yield $\alpha_s(M_Z) = 0.118 \pm 0.001 \pm 0.007$ [28] and from the CCFR neutrino experiment at Fermilab $\alpha_s(M_Z) = 0.119 \pm 0.002 \pm 0.004$ [29]. The last measurement is notable in that it represents the single most accurate measurement of α_s to date and that a long–standing discrepancy between deep inelastic scattering derivations and LEP derivations of α_s has vanished. (Previously deep inelastic scattering measurements where about three standard deviations below LEP measurements.) These latest measurements do not change the world average.

CONCLUSIONS

The vitality of QCD studies has never been greater. Recent results from the three collider and many fixed target environments have stimulated great experimental and theoretical progress. Jet production and jet characteristics are well described by perturbative QCD and are setting ever higher limits on "new" physics. Semi–inclusive measurements are providing important new clues as to the nature of higher order corrections to QCD calculations. And perhaps of a more fundamental nature, beautiful measurements of the QCD coupling constants have confirmed the correctness of SU(3) as the gauge group of strong interactions. Many other ongoing analyses will continue to explore QCD and the future remains bright with commissioning of the high luminosity Main Injector at Fermilab and high energy LHC at CERN.

REFERENCES

1. S. Abachi *et al.* (DØCollaboration), "The DØDetector", NIM A**338** 185 (1994).
2. M.Bhattacharjee, "Inclusive Jet Cross Section and Dijet Angular Distribution at DØ", Proc. of Hadron Collider Physics Conf., Stony Brook, NY (1997)
3. W.T.Giele, E.W.N.Glover, and D.A.Kosower, Nucl. Phys. B**403**, 633 (1993). Calculations performed with their program JETRAD.
4. S.Ellis *et al.* Phys. Rev. Lett **64** 2121 (1900).
5. F.Abe *et al.* (CDF Collaboration) NIM Res., Sect. **A272**, 376 (1988) and references therein.
6. F.Abe *et al.* (CDF Collaboration), Phys. Rev. Lett., **77** 438 (1996).
7. P. Melese, (CDF Collaboration), Proc. 11^{th} Les Rencontres de Physique de la Vallee D'Aosta: Results and Perspectives in Particle Physics, La Thuile, Italy, 1997. FERMILAB-CONF-97/167-E.
8. A.D.MArtin, R.G.Roberts, W.J.Stirling, Phys. Lett. **B354** 155 (1995).
9. F. Abe *et al.* (CDF Collaboration), Phys. Rev. Lett., **77** 5336 (1996).
10. M.Bhattacharjee, "Inclusive Jet Cross Sections", Proc. of DPF96, Minneapolis, MN, 1996 and FERMILAB–CONF–96/304–E.
11. F.Abe *et al.* (CDF Collaboration), Phys. Rev. Lett. **68** 1104 (1992).

12. S.Abachi *et al.* (DØCollaboration), Phys. Lett. **B357**, 500 (1995). F. Abe *et al.* (CDF Collaboration), Phys. Rev. Lett. **70** 713 1993., R.Akers *et al.* (OPAL Collaboration) Zeit. Phys. **C63** 197 (1994).
13. G.Alexander *et al.* (Opal Collaboration), Ziet. Phy. **C69** 543, (1996).
14. M.Martinez, "Jet Shapes at HERA", Proc. of 5^th Int. Workshop on Deep Inelastic Scattering and QCD, Chicago, (1997), See URL: http://www.hep.anl.gov/dis97/.
15. M.Klasen and G.Kramer, "Jet Shapes in ep and $p\bar{p}$ Collisions in NLO QCD", DESY 97-002 and hep-ph/9701247 preprints (1997).
16. W.T.Geile, E.W.N.Glover, and D.A.Kosower, Nucl,Phys. B403, 633 (1993).
17. T.Joffe–Minor "$W/Z + jets$ Production at the Tevatron", Proc. of 5^th Int. Workshop on Deep Inelastic Scattering and QCD, Chicago, (1997), See URL: http://www.hep.anl.gov/dis97/.
18. E.Laenen, J.Smith, and W.van Neerven, Phys.Lett **321**, 254 (1994). E.Berger and H.Contopangaos, Phys. Rev. D **54** 3085 (1996). S.Catani, M.L.Mangano, P.Nason, and L.Trentadue, Phys. Lett. **B378**, 329 (1996)
19. S. Krzywdzinski, "Top Cross Sections at the Tevatron", Frontiers in Contemporary Physics, Vanderbilt University, May 1997.
20. F.Stichelbaut, "Properties of $b\bar{b}$ Production at the Tevatron", Rencontres de Moriond, Les Arcs, France 1997, FERMILAB-Conf/159–E preprint.
21. F.Abe *et al.* (CDF Collaboration), Phys. Rev. Lett. **73**, 2662 (1994). S. Abachi *et al.* (DØCollaboration), Phys. Rev. Lett. **77**, 5011 (1996).
22. H.Montgomery, "Overview of Results from the Fermilab Fixed Target and Collider Experiments", Proc. of 5^th Int. Workshop on Deep Inelastic Scattering and QCD, Chicago, (1997), See URL: http://www.hep.anl.gov/dis97/ and FERMILAB-Conf–97/193 preprint.
23. J.Huston *et al.* (CTEQ Collaboration), "A Global QCD Study of Direct Photon Production", MSU–HEP–41027 and CTEQ-407 preprints, (1995).
24. F.Abe *et al.* (CDF Collaboration) Phys. Rev. Lett. **70**, 2232 (1993).
25. R.Barate *et al.*, (ALEPH Collaboration), "A Measurement of the QCD Colour Factors and a Limit on the Light Gluino", CERN-PPE/97–002 preprint (1997), Submitted to Zeit. Phys. C.
26. M.Schmelling, "Status of the Strong Coupling Constant", Proc. of the XXVIII International Conf. on High Energy Physics, Warsaw, (1996).
27. S.Marti i Garcia, "A Review of α_s Measurements at LEP", Proc. of 5^th Int. Workshop on Deep Inelastic Scattering and QCD, Chicago, (1997), See URL: http://www.hep.anl.gov/dis97/.
28. H.U.Martyn and K.Rabbertz, "Results on Event Shapes in DIS", Proc. of 5^th Int. Workshop on Deep Inelastic Scattering and QCD, Chicago, (1997), See URL: http://www.hep.anl.gov/dis97/. M.Martinez,
29. W.G.Seligman *et al.* (CCFR Collaboration), NEVIS–REPORT–292, (1997), Accepted for publication in Phys. Rev. Lett.